International Journal of Earth, Energy and Environmental Sciences
ISSN: 2517-942X
Vol:15, No:4, 2021

Early Melt Season Variability of Fast Ice Degradation Due to Small Arctic Riverine Heat Fluxes

Grace E. Santella, Shawn G. Gallaher, Joseph P. Smith

***Abstract*—**In order to determine the importance of small-system riverine heat flux on regional landfast sea ice breakup, our study explores the annual spring freshet of the Sagavanirktok River from 2014-2019. Seasonal heat cycling ultimately serves as the driving mechanism behind the freshet; however, as an emerging area of study, the extent to which inland thermodynamics influence coastal tundra geomorphology and connected landfast sea ice has not been extensively investigated in relation to small-scale Arctic river systems. The Sagavanirktok River is a small-to-midsized river system that flows south-to-north on the Alaskan North Slope from the Brooks mountain range to the Beaufort Sea at Prudhoe Bay. Seasonal warming in the spring rapidly melts snow and ice in a northwards progression from the Brooks Range and transitional tundra highlands towards the coast and when coupled with seasonal precipitation, results in a pulsed freshet that propagates through the Sagavanirktok River. The concentrated presence of newly exposed vegetation in the transitional tundra region due to spring melting results in higher absorption of solar radiation due to a lower albedo relative to snow-covered tundra and/or landfast sea ice. This results in spring flood runoff that advances over impermeable early-season permafrost soils with elevated temperatures relative to landfast sea ice and sub-ice flow. We examine the extent to which interannual temporal variability influences the onset and magnitude of river discharge by analyzing field measurements from the United States Geological Survey (USGS) river and meteorological observation sites. Rapid influx of heat to the Arctic Ocean via riverine systems results in a noticeable decay of landfast sea ice independent of ice breakup seaward of the shear zone. Utilizing MODIS imagery from NASA's Terra satellite, interannual variability of river discharge is visualized, allowing for optical validation that the discharge flow is interacting with landfast sea ice. Thermal erosion experienced by sediment fast ice at the arrival of warm overflow preconditions the ice regime for rapid thawing. We investigate the extent to which interannual heat flux from the Sagavanirktok River's freshet significantly influences the onset of local landfast sea ice breakup. The early-season warming of atmospheric temperatures is evidenced by the presence of storms which introduce liquid, rather than frozen, precipitation into the system. The resultant decreased albedo of the transitional tundra supports the positive relationship between early-season precipitation events, inland thermodynamic cycling, and degradation of landfast sea ice. Early removal of landfast sea ice increases coastal erosion in these regions and has implications for coastline geomorphology which stress industrial, ecological, and humanitarian infrastructure.

***Keywords*—**Albedo, freshet, landfast sea ice, riverine heat flux, seasonal heat cycling.

I. Introduction

EACH spring ice bound small-to-midsize Arctic rivers thaw due to meltwater runoff and warming atmospheric temperatures. This period is typically known as the spring freshet and is generally synchronized with the peak annual discharge [13]. The increase in river discharge and persistent ice jams causes extensive flooding over river banks and delta regions. The first indication of the start of the spring freshet is evident at the ocean end member as snow and ice meltwater overflows onto the landfast sea ice, prompting thermal erosion and eventual drainage through vertical flow vortices called strudel to occur [2], [15]. The erosional Arctic shoreface is dominated by sediment fast sea ice, whose outer edge breaks under the pressure of wave action, creating an active tidal crack between the sediment fast sea ice and the floating fast ice. Stability of sediment fast ice approximately follows the 2-m isobath, at which point the ice regime transitions to floating fast ice [6], [15]. The active tidal crack progresses seaward from the coastline as the sea ice grows, until the tensile strength of the fast ice is permanently exceeded by wave action, causing a separation between fast ice and floating pack ice to occur at approximately the 18 to 25-m isobath [9], [12], [15].

The separation between ice regimes allows for a baseline in order to determine whether sea ice degradation occurs via mechanical or thermodynamic forcing. Major river systems in the Arctic, including the Ob, Yenisey, Lena, Kolyma, and Mackenzie Rivers, have been credited with significant discharge resulting in thermal decay of landfast sea ice near their respective deltas [7], [8], [13]. As the atmosphere warms, the summation of small river heat influx into the Arctic Ocean is expected to have a significant influence on local sea ice breakup, like that of large rivers [14].

Reference [14] found a significant communication between air and river water temperature, and that river water temperature followed air temperature increases. The influx of terrestrial heat into the Arctic Ocean through the Sagavanirktok River originates with shortwave solar radiation absorbing inland near the Brooks Range and the transitional tundra headwaters [7], [13]. The lower albedo of the transitional tundra relative to that of sea ice results in accelerated warming of air and active-layer temperatures, and consequently, warming of the watershed river water. Understanding riverine lateral heat fluxes from these small-to-midsized rivers is fundamental to understanding melt season decline of landfast sea ice in the Western Arctic Ocean. Our aim is to identify the extent to which inland thermodynamics influence Sagavanirktok River delta geomorphology in relation to connected landfast sea ice during the annual spring freshet.

G.E. Santella, MIDN, USN, S.G. Gallaher, CDR, USN, PhD and J.P. Smith, PhD are with the United States Naval Academy, Annapolis, MD 21402, USA (e-mail: m215898@usna.edu, gallaher@usna.edu, jpsmith@usna.edu).

II. Study Area and Methods

Several publicly available data archives were integrated from 2014-2019 to include multi-spectral imagery from NASA's Aqua Earth-observing satellite MODIS instrument, Toolik Field Station Environmental Data Center temperature and precipitation data, and USGS river discharge and temperature (Fig. 1).

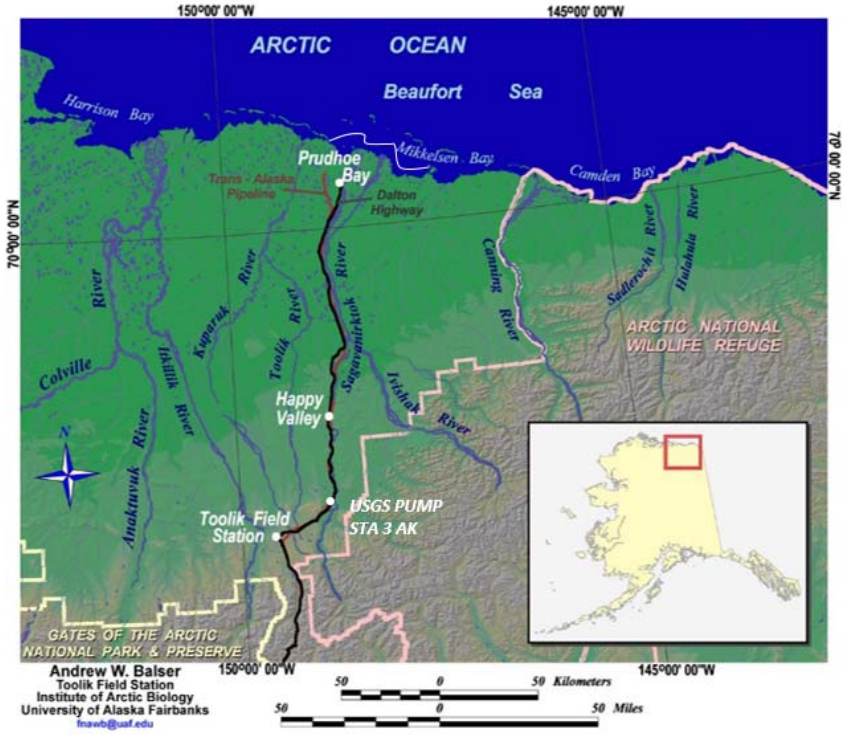

Fig. 1 Map of study site detailing Toolik Field Station, USGS PUMP STA 3 AK, and the Sagavanirktok River watershed near Prudhoe Bay. Additionally, approximate 2 m isobath for the Sagavanirktok River is detailed in white. Image provided by the Arctic Institute of Biology, University of Alaska Fairbanks [3]

MODIS Aqua satellite data are available via Worldview to provide real-time corrected reflectance images. MODIS produces a seven-band product: band 1 (620-670 nm), 2 (841-876 nm), 3 (459-479 nm), 4 (545-565 nm), 5 (1230-1250 nm), 6 (1628-1652 nm) and 7 (2105-2155 nm). To maximize the contrast between snow, ice, and clouds, we filtered the product to show only bands 7, 2, and 1. This combination takes advantage of the highly absorbent properties of snow and ice in the near infrared and short-wave infrared ranges (bands 2 and 7, respectively), and reflectivity in the visible spectrum (band 1). The result is a false color which shows thick ice/snow as a bright turquoise, and ice crystals in the clouds as a light blue/white. Because of the low albedo of liquid water, it shows up as dark blue/black on the imagery. This filter allows us to clearly see overflow and landfast sea ice breakup, at a sensor resolution of 500 m [11], [20].

For Toolik Field Station located on the transitional tundra, air temperature and relative humidity were collected by the Vaisala HMP155A air temperature and relative humidity sensor. The sensor has a temperature range of -80 °C to 60 °C, with an accuracy of +/- (0.226 - 0.0028 x temperature reading) °C for temperatures ranging -80 °C to 20 °C, and +/- (0.055 + 0.0057 x temperature reading) °C for temperatures ranging 20 °C to 60 °C. Measurements were taken from an atmospheric height of 3 m in 1-hr intervals [19]. A 3-day moving mean was then applied to air temperature measurements.

Soil temperatures were collected using a Campbell Scientific Inc. AM25T Thermocouple Multiplexer at 1-hr intervals and depths of: 0 cm, 5 cm, 10 cm, 20 cm, and 50 cm. Attached to the grounding bar of the system is a platinum resistance thermometer (PRT) which provides a baseline temperature reference for all thermocouple measurements. The heat capacity of this grounding bar reduces the temperature gradient over the length of the multiplexer, which increases accuracy of the measurements. Overall, up to 25 thermocouples are capable of being sequentially connected to a common differential channel. The thermocouple multiplexer has an internal PRT operating efficiency of +/- 0.2 °C for temperatures ranging from -25 °C to 50 °C, and +/- 0.4 °C for temperatures ranging from -40 °C to 85 °C [5]. The active layer was determined to encompass the top 10 cm, and as such these temperatures were averaged and a 3-day moving mean applied.

Annual rainfall at Toolik Field Station was measured by the Texas Electronics, Inc. TE525(WS) tipping bucket electric rain gage. This diverts rainfall from collector funnels and into a tipping bucket; for each tip, an electromagnetic response is

emitted for every 0.01 inches of rain. The mechanism is accurate to 1% for a temperature range of 0 °C to 37 °C, and 2 in/hr or less of precipitation [16]. Measurements were taken at 1-hr intervals, and no statistical manipulation took place.

Water temperature and discharge measurements for the Sagavanirktok River were gathered from USGS hydrological site 1590800 SAGAVANIRKTOK R NR PUMP STA 3 AK. This observation station is located at 69° 00' 57" N 148° 49' 04" W [17]. River temperature measurements were given as daily maximum, minimum, and mean; we analyzed the latter. At the same site, mean daily discharge was measured as a function of area of the channel cross section multiplied by the average velocity of flow in that cross section. The Acoustic Doppler Current Profile (ADCP) was used to quantify river velocity and depth. USGS stream gages measure river stage as a means to develop a stage-discharge relationship in order to create a continuous discharge record [18]. Similar to other manipulated parameters, we converted to meters and applied a 3-day moving mean to daily discharge data.

Advective heat flux through the Sagavanirktok River, H_f, is calculated relative to the freezing point of water:

$$H_f = \rho_0 C_p T Q \quad (1)$$

where ρ_0 is reference density, C_p is the heat capacity of freshwater, T is the mean daily water temperature, and Q is the mean daily discharge [10].

III. Results and Discussion

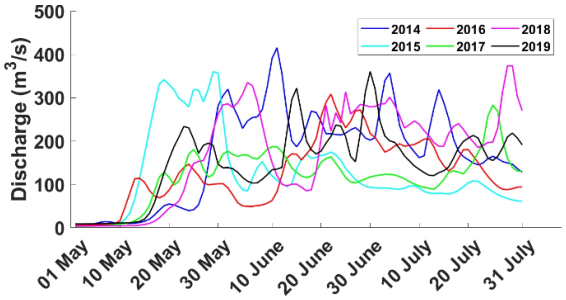

Fig. 2 Annual Sagavanirktok River discharge (m^3/s) from USGS PUMP STA 3

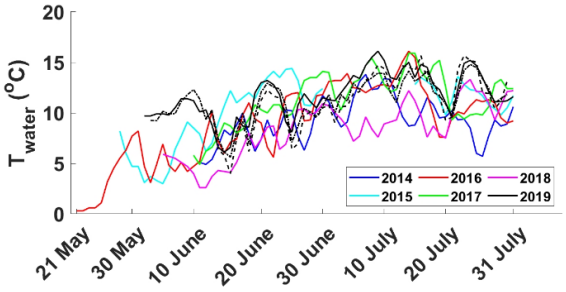

Fig. 3 Sagavanirktok river mean water temperature (°C). In addition to USGS data, supplementary data was provided by Alaska North Slope Material Flux Study (AKMFS) and shows temperature of tundra streams (- -) and the Sagavanirktok River (-.)

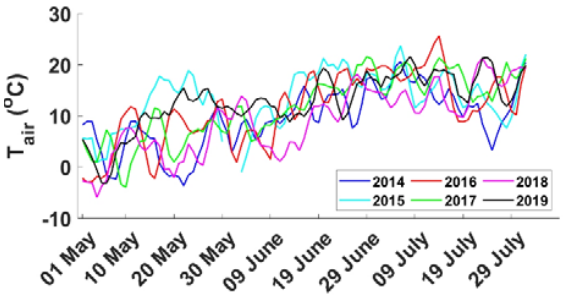

Fig. 4 Comparison of annual mean air temperature (°C) from 3-m at Toolik Field Station

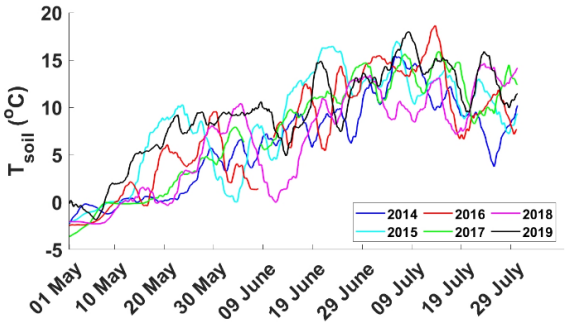

Fig. 5 Mean active layer temperature (°C) for the top 10 cm at Toolik Field Station

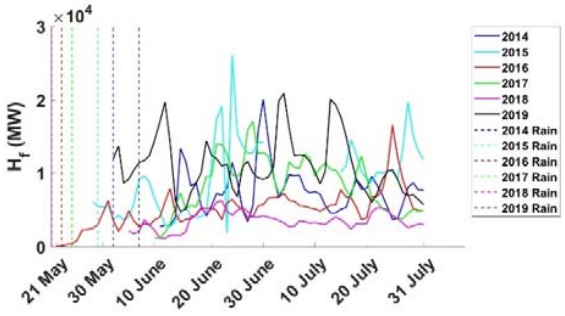

Fig. 6 Total heat flux (MW) through the Sagavanirktok River, overlaid with early-season precipitation events over a 24-hr time period. 31 May-01 June 2014 measured 11.176 mm; 29 May 2015 measured 32.258 mm; 21 May – 22 May 2016 measured 9.398 mm; 23 May – 24 May 2017 measured 6.463 mm; 17 May 2018 measured 12.083 mm; 06 June 2019 measured 10.397 mm. Total daily precipitation (mm) from Toolik Field Station

Five different parameters were studied to determine the influence small riverine heat fluxes have on landfast sea ice breakup: discharge; water temperature; 3-m air temperature; 0-10 cm average soil temperature; and precipitation (Figs. 2-6). Additionally, discharge overflow and open water area (km^2) for the Sagavanirktok River delta were estimated via MODIS imagery (Fig. 7). MODIS imagery also facilitated the determination of an annual average date for river discharge overflow and complete fast ice retreat during the study period as 12 May and 02 July respectfully (Figs. 8-13). By analyzing the magnitude of rain introduced to the system, the timing of

precipitation events, and periods of high riverine heat flux, it was determined that for an early-season rain event to significantly impact the warming of the system in the 2014-2019 study period, it must occur within 20 May – 06 June and introduce an estimated minimum of 10.00 mm of rain to the system. The average residence time for a parcel of water flowing through the Sagavanirktok River watershed, 8.67 days, is represented as the time between the significant precipitation event and subsequent heat flux increase (Fig. 6).

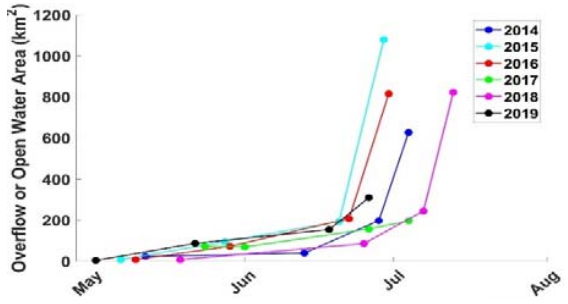

Fig. 7 Estimated discharge overflow and open water area (km^2) for the Sagavanirktok River delta

A. 2014 Breakup

Spring freshet conditions began as early as 12 May on the Sagavanirktok River, as evidenced by MODIS imagery (Fig. 8 A). On 11 June, peak seasonal discharge is measured 458.73 m^3/s at USGS PUMP STA 3 (Fig. 2). Two days later, noticeable landfast ice decline, separate from that of mechanically-induced breakup seaward of the stable fast ice regime, became evident (Fig. 8 B). Water, air, and active layer temperatures reached seasonal maximum values at Toolik Field Station on 30 June and were recorded as 13.0 °C, 18.8 °C, and 18.59 °C respectively (Figs. 3-5). A measured value of 11.176 mm of rain was introduced into the system at Toolik Field Station on 31 May – 01 June (Fig. 6). When considering the previously discussed time delay experienced by the system between precipitation events and increasing heat flux, it is likely that this event accounted for the early season open water expanse forming at the watershed (Figs. 6, 7, and 8 B). Rising inland water, air, and active layer temperatures worked to intensify the transfer of heat into the Arctic Ocean via the Sagavanirktok River. Sediment fast ice within the 2 m isobath released as heat influx increased (Figs. 8 B and C). When MODIS imagery for the days of the noted initial spring freshet and the peak inland temperatures are compared, it becomes apparent that thermal breakup of landfast sea ice is supported by increasing heat flux through the Sagavanirktok River (Figs. 8 A and C). Complete retreat of seasonal landfast sea ice occurred on approximately 04 July, 53 days after the initial freshet was observed (Fig. 8 D).

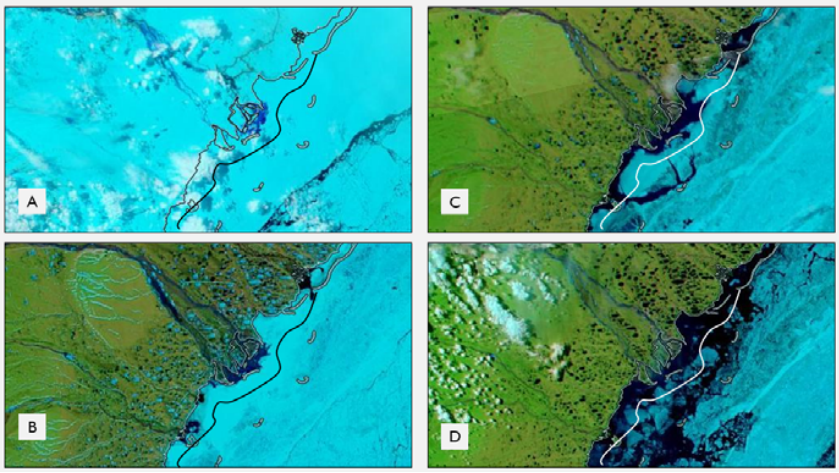

Fig. 8 Sagavanirktok River watershed and approximate 2m isobath, 2014. A) 12 May; B) 13 June; C) 28 June; D) 04 July

B. 2015 Breakup

Spring overflow from the Sagavanirktok River became evident as early as 07 May (Fig. 9 A). The uniform distribution of overflow spanning between Egg Island and Tigvariak Island preconditioned the region for thermal decay by acting to lower the local albedo and provide a conduit for lateral heat transfer across the ice surface (Fig. 9 B). On 29 May, the first peak discharge measured 467.23 m^3/s at USGS PUMP STA 3 (Fig. 2). Noticeable landfast ice breakup within the watershed aligns with this discharge event (Figs. 7 and 9 B). The first peak discharge and subsequent early-season landfast ice loss was induced by a total of 32.26 mm of rain that entered the system at Toolik Field Station on 29 May (Fig. 6). The season's second peak discharge was recorded at USGS PUMP STA 3 as 181.79 m^3/s on 23 June. Furthermore, this discharge event is directly followed by seasonal maximums at Toolik Field Station for active layer temperature, measuring 24.09 °C on 24 June, and water temperature measuring 16.0 °C on 25 June (Figs. 5 and 3). Intensifying riverine heat flux supported rapid breakup of landfast sea ice between 20-29 June (Figs. 7, and 9 C and D). It is likely that precipitation events precondition the system to be more vulnerable to the effects of thermal cycling by lowering the albedo throughout the transitional tundra. A positive correlation exists between inland thermodynamic cycling and consequential sea ice loss due to riverine heat flux in the

aftermath of precipitation events (Fig. 7).

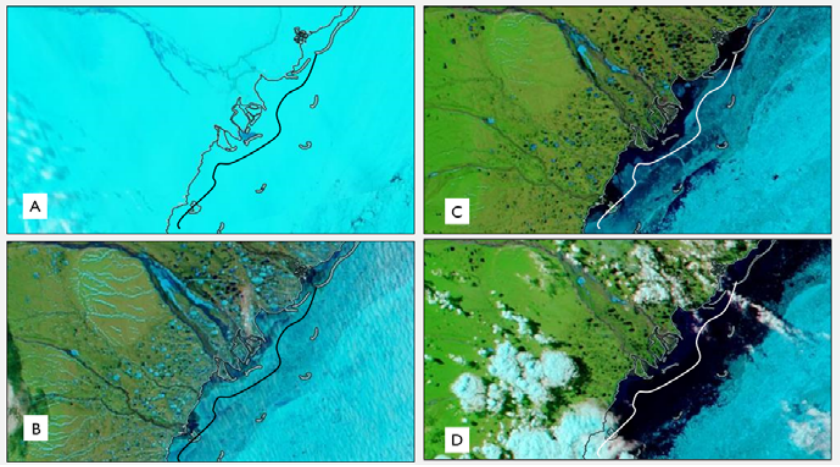

Fig. 9 Sagavanirktok River watershed and approximate 2m isobath, 2015. A) 07 May; B) 28 May; C) 20 June; D) 29 June

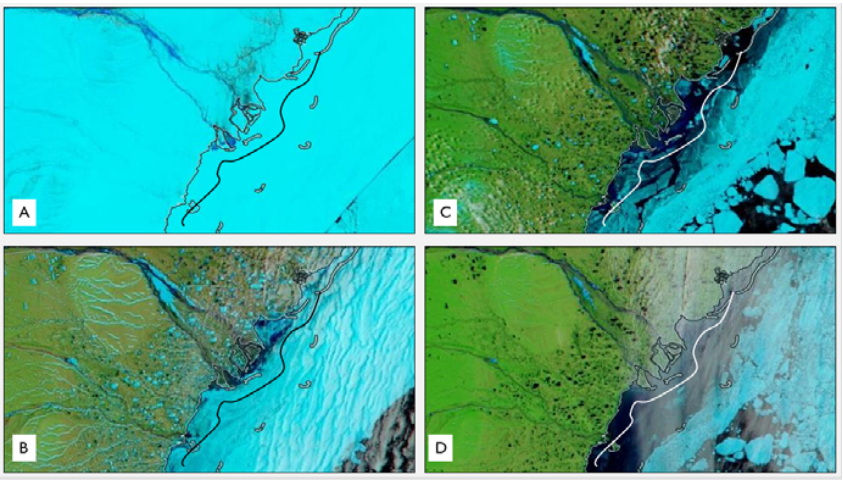

Fig. 10 Sagavanirktok River watershed and approximate 2m isobath, 2016. A) 10 May; B) 29 May; C) 22 June; D) 30 June

C.2016 Breakup

Spring freshet conditions became highly visible on 10 May, as shown by MODIS imagery. Mechanical forcing seaward of the stable fast ice regime is identified by a crack in the floating fast ice, which is visible on 10 May (Fig. 10 A). A similar phenomenon occurred in 2014 (Fig. 8 A). Notably, a rain event introduced 9.398 mm of water to the system at Toolik Field Station on 21 May – 22 May, resulting in a rapid increase of early-season riverine heat flux (Fig. 6). A seasonal maximum air temperature of 23.4 °C and a maximum active layer temperature of 23.5 °C were recorded on 17 June at Toolik Field Station (Figs. 4 and 5). The peak discharge of 2016 was measured at USGS PUMP STA 3 to be 336.97 m^3/s on 21 June (Fig. 2). Immediately following the inland heating and discharge events, a significant open water area within the 2 m isobath is observed (Figs. 7 and 10 C). Water temperature measured at USGS PUMP STA 3 steadily increased during this time and reached a maximum value of 13.6 °C on 30 June (Fig. 4). The peak water temperature aligns with the noticeable complete release of remaining landfast sea ice (Fig. 10 D). Diminishing terrestrial and riverine ice cause the system to absorb heightened levels of solar radiation, resulting in increased water temperatures and overall heat flux into the Arctic Ocean, as evidenced by the rapid retreat of landfast sea ice (Figs. 7 and 10). Significantly, there is a band of sea ice spanning from Reindeer Island past Narwhal Island which remains stable and acts as a transition point between mechanical ice breakup from the open ocean, and thermal ice breakup from the Sagavanirktok River discharge (Fig. 10 D).

D.2017 Breakup

Overflow from the Sagavanirktok River occurred on 24 May, approximately 12 days later than the previously determined average date of freshet for 2014-2019 (Fig. 11 A). Yearly maximum discharge was measured to be 200.43 m^3/s at USGS PUMP STA 3 on 25 May (Fig. 2). The failure of the spring freshet to fully develop is indicated by a significantly low maximum seasonal discharge and the persistence of landfast sea

ice within the 2 m isobath as late as 25 June (Figs. 2, 7, and 11 C). The system lacked a significant early-season precipitation event between 20 May – 06 June, and thus lacked substantial terrestrial runoff to prompt an influential freshet (Fig. 6). At Toolik Field Station, a peak active layer temperature of 21.95 °C was recorded on 27 June, closely followed by peaks in water temperature, measured as 15.9 °C at USGS PUMP STA 3, and air temperature at Toolik Field Station, measured as 24.2 °C, on 30 June (Figs. 5, 4, 3). The absence of a substantial heat flux allowed fast ice to remain near Tigvariak Island past 04 July, at which point all remaining ice is broken up mechanically (Figs. 6 and 11 D). From 25 June – 04 July, forcing from the Beaufort Gyre is recognized in the form of northwestward ice migration towards Utqiagvik on MODIS imagery (Figs. 11 C and D).

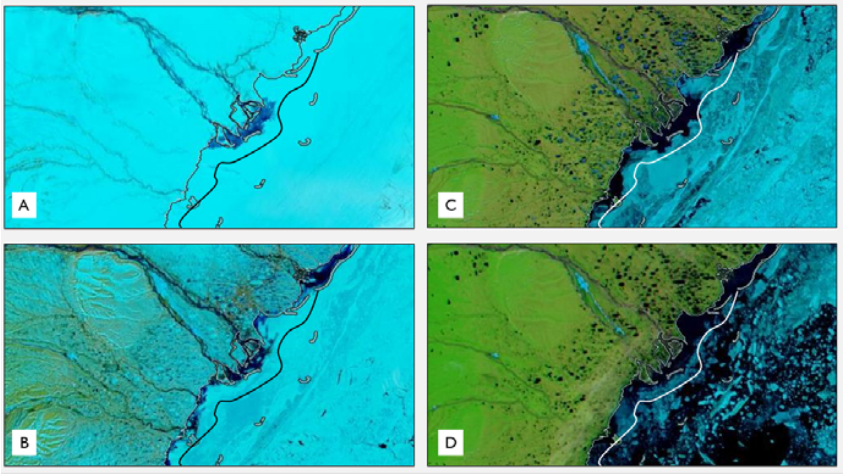

Fig. 11 Sagavanirktok River watershed and approximate 2m isobath, 2017. A) 24 May; B) 01 June; C) 25 June; D) 04 July

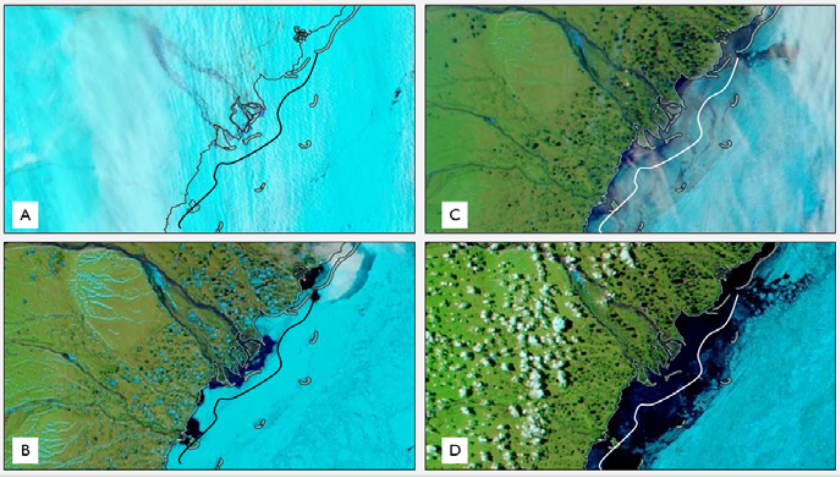

Fig. 12 Sagavanirktok River watershed and approximate 2m isobath, 2018. A) 19 May; B) 25 June; C) 07 July; D) 13 July

E. 2018 Breakup

Spring overflow conditions became visible on 19 May, as seen on MODIS imagery (Fig. 12 A). Maximum seasonal discharge measured 436.08 m^3/s at USGS PUMP STA 3 on 24 June (Fig. 2). At Toolik Field Station, a peak active layer temperature of 21.6 °C was measured on 26 June, closely followed by an air temperature of 19.5 °C on 27 June (Figs. 4 and 5). A river water temperature of 11.9 °C was measured at USGS PUMP STA 3 on 30 June (Fig. 3). Complete release of landfast sea ice occurred around 13 July (Fig. 12 D). The 2018 ice regime in the Western Arctic is characterized by the persistence of floating pack ice seaward of the shear zone, like what was observed in the 2014 and 2015 seasons (Figs. 8, 9, 12). Thermodynamic influence on landfast sea ice breakup is apparent in the absence of mechanical forcing. Notably, no significant precipitation event was recorded during the study period to act to accelerate early-season warming (Fig. 6). A storm on 17 May introduced 12.083 mm of rain to the system, however 23 days elapsed before heat flux through the Sagavanirktok River experienced a noticeable increase on 09 June. This 17 May precipitation event occurred outside of the determined ideal window for significant heat cycling to occur as a result of rain being introduced. It is likely that the system lacked the ability to transfer substantial heat across the air-river

interface until obstructions to hydraulic connectivity, primarily in the form of riverine ice dams, could be broken down. Such significant heat transfer is present in the 2014, 2015, 2016, and 2019 seasons (Fig. 6).

F. 2019 Breakup

Spring freshet conditions were first observed as early as 02 May, as shown by MODIS imagery (Fig. 13 A). Seasonal peak river water temperature was recorded as 14.3 °C on 21 June at USGS PUMP STA 3 (Fig. 3). The maximum values for air temperature, measured as 21.4 °C at Toolik Field Station, active layer temperature, measured as 22.52 °C also at Toolik Field Station, and discharge, measured as 410.59 m^3/s at USGS PUMP STA 3, were recorded on 30 June (Figs. 3, 5, 2). Notably, landfast sea ice retreated from the coast completely as early as 26 June (Fig. 13 D). The maximum discharge rate was measured after the ice had retreated, however river temperature peaked four days prior. We note the occurrence of a storm on 06 June which introduced 10.397 mm of rain to the system (Fig. 6). A 5-day residence time was experienced before heat flux experienced a local peak, which is below the average residence time when compared to 2014, 2015, and 2016 (Fig. 6). Previously heightened river water temperatures suggest lower levels of river ice, and thus allow for accelerated lateral heat transfer through the system (Figs. 3 and 13). The presence of heat within the river, measured to be 17,119.2 MJ on 11 June, as discharge increased ultimately worked to degrade landfast sea ice by purely thermodynamic means, rather than a combination of thermodynamic and mechanical forcing from the flow of the Sagavanirktok River. Mechanical forcing from the Sagavanirktok River is typically insignificant when compared to the magnitude of those found in the marginal ice zone of the Western Arctic.

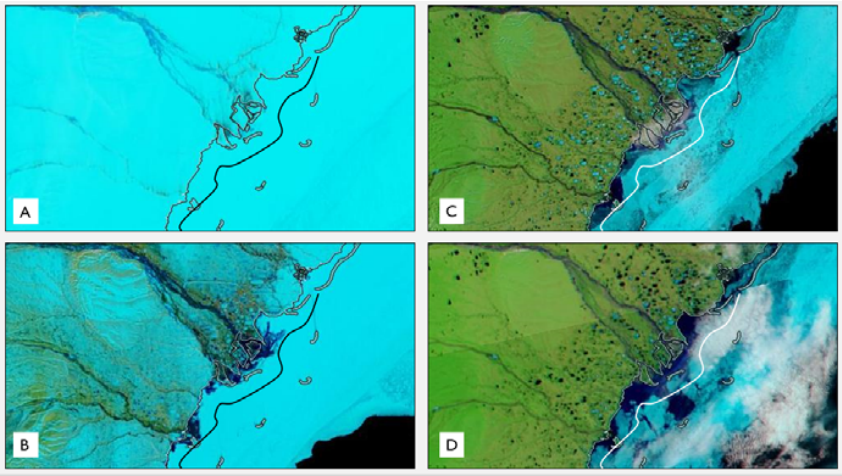

Fig. 13 Sagavanirktok River watershed and approximate 2m isobath, 2019. A) 02 May; B) 22 May; C) 18 June; D) 26 June

IV. Conclusion

On average, maximum air temperatures will precede maximum river water temperatures [2]. 2019 is the sole year within the study period where river water temperature led air temperature. As air temperature increased, it was observed that river water temperatures cooled slightly before responding to increased solar radiation, in the manner described by [2]. Inland precipitation events are credited with facilitating this temperature phenomena.

We identified a positive relationship between rain events, terrestrial warming, and subsequent sea ice loss. The 2014, 2015, 2016, and 2019 seasons showcase the role of rain events as a significant factor which precondition the system for enhanced early-season warming correlating to rapid release of landfast sea ice. Precipitation events act to accelerate the green-up of the transitional tundra, as seen in 2014, 2015, 2016, and 2019; however, for an early-season rain event to significantly impact the warming of the system, it must occur within the approximate two-week span between 20 May – 06 June and introduce a minimum of approximately 10.00 mm of rain to the system. Decreased albedo following precipitation events allows for net absorption of solar radiation to warm the system, beginning by raising air temperatures.

The 2017 season lacks a distinguishable freshet despite the presence of temperatures comparable to previous study years. Significantly, no substantial precipitation event occurred in 2017, with the largest early-season storm yielding less than determined 10.00 mm minimum requirement for significant influence to occur. The misalignment of heat cycling combined with the lack of a preconditioning agent in the form of a precipitation event resulted in an absence of thermal sea ice decay.

It can be confidently determined that thermodynamic cycling ultimately acts independent of precipitation when considering a year which had dominant thermal landfast sea ice breakup, yet lacked a significant rain event, such as in 2018 when the only early-season storm occurred outside of the determined window for influence on heat flux to occur as a result. Although seasonal heat cycling has the capacity to function effectively to degrade landfast sea ice independently of inland precipitation, when occurring in tandem, these two mechanisms act to accelerate thermal erosion of the sea ice.

The Sagavanirktok River functions as a crucial source of heat for the Prudhoe Bay region and local coastline. The introduction of riverine heat to landfast sea ice accelerates early-season ice breakup. The transportation of heat into the ocean historically has been predictable in the early summer, allowing indigenous peoples the security of traditional knowledge to aid a subsistence lifestyle, and for oil companies to confidently place secure pipelines [1]. The early-season warming of atmospheric temperatures due to global warming is evidenced by the presence of storms which introduce liquid, rather than frozen, precipitation into the system [4]. The resultant decreased albedo of the transitional tundra supports a potentially important positive relationship between early-season precipitation events, inland thermodynamic cycling, and breakup of landfast sea ice. The early removal of landfast sea ice by the Sagavanirktok River has the potential to increase coastal erosion in these regions and has cascading implications to the coastline geomorphology which stress industrial, ecological, and humanitarian infrastructure.

ACKNOWLEDGMENTS

Sagavanirktok River water temperature and discharge rate data were provided courtesy of the U.S. Geological Survey. We acknowledge the use of imagery from the NASA Worldview application, part of the NASA Earth Observing System Data and Information System (EOSDIS). Annual precipitation, air temperature, and soil temperature data sets were provided by the Toolik Field Station Environmental Data Center. Toolik Field Station data is based upon work supported by the National Science Foundation under grant #1623461. Finally, we acknowledge the use of tundra stream water temperature and Sagavanirktok River water temperature data sets from the Alaska North Slope Material Flux Study. This material is based upon work supported by the Strategic Environmental Research and Development Program grant #RC19-1382.

REFERENCES

[1] Abdalla, B., Jukes, P., Eltaher, A., and Duron, B., 2008, The Technical Challenges of Designing Oil and Gas Pipelines in the Arctic: *OCEANS 2008*, Quebec City, QC, Canada, 2008, pp. 1-1, doi: 10.1109/OCEANS.2008.5151914.

[2] Are, F., Reimnitz, E., Grigoriev, M., Hubberten, H.-W., and Rachold, V., 2008, The Influence of Cryogenic Processes on the Erosional Arctic Shoreface: Journal of Coastal Research, vol. 24, no. 1, pp. 110-121.

[3] Balser, A.W. (n.d.), *Toolik Field Station to Prudhoe Bay/Deadhorse ALASKA* (map). (1:500,000). Institute of Arctic Biology, University of Alaska Fairbanks.

[4] Box, J.E. and 19 others, 2019, Key indicators of Arctic climate change: 1971-2017: Environmental Research Letters, vol. 14, no. 4, doi: 10.1088/1748-9326/aafc1b.

[5] Campbell Scientific, Inc., AM25T 25-Channel Solid-State Thermocouple Multiplexer homepage: https://www.campbellsci.com/am25t, accessed 13 February 2021.

[6] Dammann, D.O., Eriksson, L.E.B., Mahoney, A.R. Stevens, C.W., Sanden, J., Eicken, H., Meyer, F.J., and Tweedie, C.E., 2018, Mapping Arctic Bottomfast Sea Ice using SAR Interferometry: Remote Sensing, vol. 10, no. 720.

[7] Dean, K.G., Stringer, W.J., Ahlnäs, K., Searcy, C., and Weingartner, T. (1994), The influence of river discharge on the thawin go fsea ice, Mackenzie River Delta: albedo and temperature analyses: Polar Research, vol. 13, no. 1, pp. 83-94, doi: 10.3402/polar.v13i1.6683.

[8] Georgiadi, A.G., Kashutina, E.A., and Milyukova, I.P. (2018), Long-term Changes of Water Flow, Water Temperature and Heat Flux of the Largest Siberian Rivers: Polarforschung, vol. 87, no. 2, pp. 167-176.

[9] Mahoney, A., Eicken, H., Gaylord, A.G., and Shapiro, L., 2007, Alaska landfast sea ice: Links with bathymetry and atmospheric circulation: Journal of Geophysical Research, vol. 112, doi: 10.1029/2006JC003559

[10] McPhee, M.G., *Air-Ice-Ocean Interaction: Turbulent Ocean Boundary Layer Exchange Processes,* 2008, 2nd Ed., New York Springer. https://doi.org/10.1007/978-0-387-78335-2

[11] NASA Earth Observing System Data and Information System (n.d.). NASA Worldview. https://worldview. earthdata.nasa.gov

[12] Nghiem, S.V., Hall, D.K., Rigor, I.G., Li, P., and Neumann, G., 2014, Effects of Mackenzie River discharge and bathymetry on sea ice in the Beaufort Sea: Geophysical Research Letters, vol. 41, pp. 873-879.

[13] Park, H., and 7 others, 2020, Increasing riverine heat influx triggers Arctic sea ice decline and oceanic and atmospheric warming: Science Advances, vol. 6, doi: 10.1126/sciadv.abc4699

[14] Park, H., Yoshikawa, Y., Yang, D., and Oshima, K., 2017, Warming Water in the Arctic Terrestrial Rivers under Climate Change: Journal of Hydrometeorology, pp. 1983- 1995, doi: 10.1175/JHM-D-16-0260.1.

[15] Reimnitz, E., 2000, Interactions of River Discharge with Sea Ice in Proximity of Arctic Deltas: A Review: Polarfoschung, vol. 70, pp. 123-134.

[16] Toolik Field Station Environmental Data Center, Current Met Station Components: https://toolik.alaska.edu/edc/abiotic_monitoring/instrumentation.php, accessed 13 February 2021.

[17] United States Geological Survey, USGS 15908000 SAGAVANIRKTOK R NR PUMP STA 3 AK: https://waterdata.usgs.gov/nwis/uv/?site_no=15908000&agency_cd=USGS&referred_module=sw, accessed August 2020.

[18] United States Geological Survey (n.d.). *How Streamflow is Measured*. https://www.usgs.gov/ special-topic/water-science-school/science/how-streamflow-measured?qt-science_center_objects=0#qt-science_center_objects, accessed August 2020.

[19] Vaisalla, HUMICAP Humidity and Temperature Probe HMP155 https://www.vaisala.com/sites/default/files/documents/HMP155-Datasheet-B210752EN.pdf, accessed 13 February 2021.

[20] Vermote, E.F., Roger, J.C., and Ray, J.P., 2015, MODIS Surface Reflectance User's Guide, collection 6, version 1.4, http://modis-sr.ltdri.org.